Electronic Supplementary Information

Integration of Yolk–Shell Units into Robust and Highly Reactive Nanoreactor: A Platform for Cascade Reactions

Yingchun Guo,[a] Lei Feng,[a] Xiaomei Wang[a], Xu Zhang*[a,b]*

[a] *School of Chemical Engineering and Technology, Hebei University of Technology, Tianjin 300130, P.R. China. Email address: xmwang@hebut.edu.cn; xuzhang@hebut.edu.cn; Tel/Fax: +86 022 60200443*

[b] *National-Local Joint Engineering Laboratory for Energy Conservation of Chemical Process Integration and Resources Utilization*

*Corresponding author: E-mail: xmwang@hebut.edu.cn and xuzhang@hebut.edu.cn

Experiment

Materials:

Tetraethoxysilane (TEOS, 99.5%), hydrofluoric acid (HF, 48 wt%), and concentrated sulfuric acid (H_2SO_4, 98 wt%) were purchased from Tianjin Fuchen Chemical Reagent Company. Trimethylsilyl iodide (Me_3SiI, 97%), nitromethane (98.5%, GC), benzaldehyde dimethyl acetal (BDA, 98%), 4-nitrobenzaldehyde, 1,2-phenylenediamine, ethyl cyanoacetate, palladium chloride, and di-*tert*-butyl dicarbonate ($(Boc)_2O$, 98%) were purchased from Aladdin Industrial Corporation. *p*-aminostyrene (St-NH_2, 96%) was received from J&K Chemical Company. Styrene (St) and divinylbenzene (DVB, containing 80% divinylbenzene isomers) were obtained from Tianjin Guangfujingxi Chemical Company. St and DVB monomers were purified by distillation under reduced pressure and stored nitrogen atmosphere before their polymerization. The Boc-*p*-aminostyrene (St-NHBoc) monomer, which was synthesized by the chemical reaction between St-NH_2 monomer and $(Boc)_2O$ according to Covolan et al.[1] All other reagents were used as received.

Preparation of CLPS@SiO_2 CS-CCTs

First, the synthesis of monodisperse CLPS microspheres with controlled diameter about 238 nm (PDI=0.019) was carried out by emulsion polymerization method reported previously.[2] Then 1.0 g the CLPS microspheres were immersed in large quantity of concentrated sulfuric acid (40 mL) at 25 °C for 3 h and then heated to 40 °C for 12 h under slow stirring to

derive sulfonated CLPS microspheres. The obtained CLPS-SO_3H microspheres were washed with ultrapure water until neutral. The freeze-dried CLPS-SO_3H microspheres (0.5 g) were dispersed into excessive TEOS/ethanol (10 mL/50 mL) mixture for 2 h at 25 °C under mechanical stirring. Then ultrapure water (10 mL) was added to the mixture at 25 °C for 24 h to form silica partially covered CLPS-SO_3H microspheres via first sol-gel process. Then the resulting CLPS-SO_3H@SiO_2 microspheres were centrifuged and washed three times with ethanol, and dispersed in ethanol (250 mL) under sonication. TEOS (5 mL) and ammonia solution (15 mL) were sequentially added into the reaction mixture. The reaction occurred at 25 °C for 12 h under slow stirring via the second sol-gel process. The purpose of two-step reaction is to form a thicker silica shell on the CLPS-SO_3H surface. Then the thickened CLPS-SO_3H@SiO_2 core-shell microspheres were centrifuged and washed three times with ethanol. The CLPS-SO_3H@SiO_2 colloidal dispersions were ultrasonicated to form a uniform emulsion and then centrifuged at 1000 rpm for 12 h. The obtained precipitations were then dried at room temperature for 5 days to obtain the final monolithic CLPS-SO_3H@SiO_2 CS-CCTs.

Fabrication of IY-SO_3H@S-NH_2

The copolymerization solution containing St-NHBoc (9.0 g), AIBN (0.05 g) and DVB (1.0 g) was infiltrated into the voids inside the CLPS-SO_3H@SiO_2 CS-CCTs. Then polymerization reaction was carried out at 85 °C for 24 h. The as-synthesized IY-SO_3H@SiO_2/S-NHBoc composites were completely immersed into aqueous HF (5 wt%) to selectively etch the middle silica layer. After being washed with ultrapure water until neutral, the samples were ambiently dried. The as-prepared IY-SO_3H@S-NHBoc composites (1 equiv. of amine determined by elemental analysis) were treated with 1 equiv. of Me_3SiI in dry acetonitrile solution at 40 °C for 12 h under magnetic stirring. When the reaction was complete 3 equiv. of methanol was added. The deprotected samples were collected by filtration, washed with dry acetonitrile, and dried under vacuum. Thus, the IY-SO_3H@S-NH_2 was prepared.

Preparation of IY-SO_3H@S-NH_2/Pd

Pd NPs were loaded into the obtained IY-SO_3H@S-NH_2 via an in-situ reduction method. Typically, 100 mg of IY-SO_3H@S-NH_2 was immersed in 20 mL of deionized water via magnetic stirring. After stirring for 30 min at 30 °C, 12.0 mL of fresh $PdCl_2$ aqueous solution with a concentration of 1.0 mg/mL was dropwise slowly and then kept at 30 °C with stirring for 10 h. Then 2.0 mL of 0.1 M freshly prepared $NaBH_4$ aqueous solution was added dropwise, and the mixture was aged for 24 h. The creamy white color transformed into gray black. The mixture was filtered and the black powder product was washed with deionized water and ethanol several times. After drying in an oven at 60 °C overnight, the palladium-loaded products IY-SO_3H@S-NH_2/Pd was obtained.

Synthesis of 3DOM CLPS-NH_2

For comparison, various multifunctional nanoreactors with comparable acid sites and/or basic sites concentration, that is, IY-SO_3H@S-NHBoc (-SO_3H groups in the yolk and -NHBoc groups in the interconnected shell), CLPS-SO_3H microspheres (the microspheres with -SO_3H groups), 3DOM CLPS-NH_2 (the -NH_2 groups on the pore wall of 3DOM CLPS), IY-SO_3H@S (only the -SO_3H groups in the yolk), IY@S-NH_2 (only the -NH_2 groups in the interconnected shell), and 3D-IYS (without functionalities), were also prepared. SiO_2 CCTs with an average diameter of ca. 300 nm was synthesized adopting the procedures described in the literature.[3] The synthesis of 3DOM CLPS-NH_2 was almost the same as that of IY-SO_3H@S-NH_2 described above except with a change of the CCTs. For 3DOM CLPS-NH_2, the SiO_2 CCTs was used in place of the CLPS-SO_3H@SiO_2 CS-CCTs in the infiltration process.

Synthesis of IY-SO_3H@S

The synthesis of IY-SO_3H@S was almost the same as that of IY-SO_3H@S-NH_2 described above except with a change of the copolymerization solution. For IY-SO_3H@S, the monomer (St) was used in place of the monomer (St-NHBoc) in the copolymerization process.

IY@S-NH_2 and IY@S

The monodisperse CLPS-PVP@SiO_2 core-shell microspheres were prepared by emulsion polymerization and subsequent sol-gel process that was slightly modified from previously reported methods.[4] CLPS-PVP@SiO_2 core-shell microspheres were centrifuged at 1000 rpm for 13 h to form the CLPS-PVP@SiO_2 CS-CCTs, then allowed to air-dry. The synthesis of IY@S-NH_2 and IY@S both used these CS-CCTs. The St-NHBoc and St were used as the monomers in the copolymerization process, respectively.

The concentrations of the sulfonic acid and amine group determination by the acid-base back-titrations method.[5,6]

In order to quantify the alkalinity, 50 mg of IY-SO_3H@S-NH_2 was impregnated in an HCl solution (10 mL, 0.02 M). After 2 h of stirring at room temperature, the mixture was filtrated and washed with deionized water (3x10 mL). The obtained filtrate was titrated by a NaOH solution (0.01 M), using phenolphthalein as the indicator. In order to quantify the acidity, 50 mg of IY-SO_3H@S-NH_2 was impregnated in a KCl solution (8 mL, 0.01 M solution). After 2 h of stirring at room temperature, the mixture was filtrated and washed with deionized water (3x10 mL). The obtained filtrate was titrated by a NaOH solution (0.01 M), using phenolphthalein as the indicator. The amount of sulfonic acid and amine groups were calculated with the following formula.

$$C_{-NH2} = \frac{C(HCl) \times V(HCl) - C(NaOH) \times V(consume, NaOH)}{m(solid)}$$

$$C_{-SO3H} = \frac{C(NaOH) \times V(consume, NaOH)}{m(solid)}$$

One-pot deacetalization-Henry reaction catalyzed by IY-SO_3H@S-NH_2

For one-pot deacetalization-Henry reaction, a mixture of IY-SO_3H@S-NH_2 (1.8 mg, 0.0045 mmol of amine), nitromethane (3 mL), BDA (37.5 μL, 0.25 mmol) and water (0.2 mL) were vigorously stirred at 90 °C for 12 h under N_2 in a sealed glass vessel. To make the reaction time profiles, 100 μL of the mixture was removed with a filter syringe at different time intervals. Then the obtained products were thoroughly evaluated by GC-MS to determine the yield of benzaldehyde and *β*-nitrostyrene. For the recycling test, the catalyst was collected by filtration after the reaction and washed with CH_3NO_2 several times.

One-pot deacetalization-Knoevenagel reaction catalyzed by IY-SO_3H@S-NH_2

For one-pot deacetalization-Knoevenagel condensation reaction, a mixture of IY-SO_3H@S-NH_2 (0.032 mmol of amine), anhydrous toluene (5 mL), BDA (0.5 mmol), ethyl cyanoacetate (0.6 mmol), and water (50 μL) were vigorously stirred at 80 °C for 1.5 h, and the reaction was stopped by cooling to room temperature. The catalyst was separated via filtration and the reaction filtrate was analyzed by GC-MS.

Synthesis of the 2-(4-aminophenyl)-1*H*-benzimidazole using IY-SO_3H@S-NH_2/Pd

60 mg of IY-SO_3H@S-NH_2/Pd was dispersed in 5 mL of methanol, followed by the addition of 0.5 mmol of 4-nitrobenzaldehyde and 0.6 mmol of 1,2-phenylenediamine. The resulting mixture was stirred at 80 °C under air atmosphere for 5 h and then transferred into a Teflon-lined pressure vessel without any separation or extraction. The vessel was then pressurized with H_2 to 2 bar reacting for 8 h. After the reaction, the IY-SO_3H@S-NH_2/Pd was separated by filtration, thoroughly washed with methanol, and then reutilized as the catalyst in subsequent runs under identical reaction conditions. The yield of the product was analyzed by GC-MS.

Characterization

Fourier transform infrared (FT-IR) spectra were recorded between 4000 and 400 cm^{-1} on a Bruker VECTOR-22 spectrometer with potassium bromide (KBr) pellets. C, H, S, and N elemental analyses were performed on a Flash EA 1112 apparatus. UV-Raman spectra were recorded on a Renishaw inVia Reflex UV Raman spectrometer. The ^1H NMR spectra were registered in $CDCl_3$ by using a Bruker 400 spectrometer. X-Ray

photoelectron spectroscopy (XPS) measurements were conducted by using a Thermo Scientific ESCALab250Xi spectrometer with monochromatic Al Kα radiation (1486.6 eV) and spot size 650 μm. The binding energies were calibrated using the C 1s peak at 284.6 eV. Scanning electron microscopy (SEM) images were obtained on FEI Nova Nano-SEM450 with a concentric backscattered retractable (CBS) detector field-emission scanning electron microscope at different accelerating voltages. Transmission electron microscopy (TEM) was carried out on a JEM-2100F electron microscope running at 200 kV. Hydrodynamic diameter was acquired from Nano-ZS90 (Malvern Zetasizer). The inorganic content of the CLPS-SO_3H@SiO_2 core-shell microspheres was derived by Thermogravimetric analysis (TA, SDT-Q600). The sample was heated from ambient temperature to about 800 °C, with a heating rate of 10 °C/min, in dry flowing air. The obtained liquid solution after cascade reaction was analyzed by GC-MS using nitrobenzene as internal standard (GC-2010 Plus gas chromatograph equipped with a flame ionization detector working at 220 °C and a 30 m BPX 5 column). The injected samples were heated from 40 to 280 °C at a heating rate of 10 °C /min. The Pd contents in the IY-SO_3H@S-NH_2/Pd samples were measured with an Optima 5300DV inductively coupled plasma atomic emission spectroscopy (ICP-AES) (Perkin-Elmer). Three-dimensional morphology was investigated by atomic force microscopy (AFM) with a dimension 2 μm instrument (MultiMode 8, Bruker). Images were acquired under ambient conditions in ScanAsyst mode.

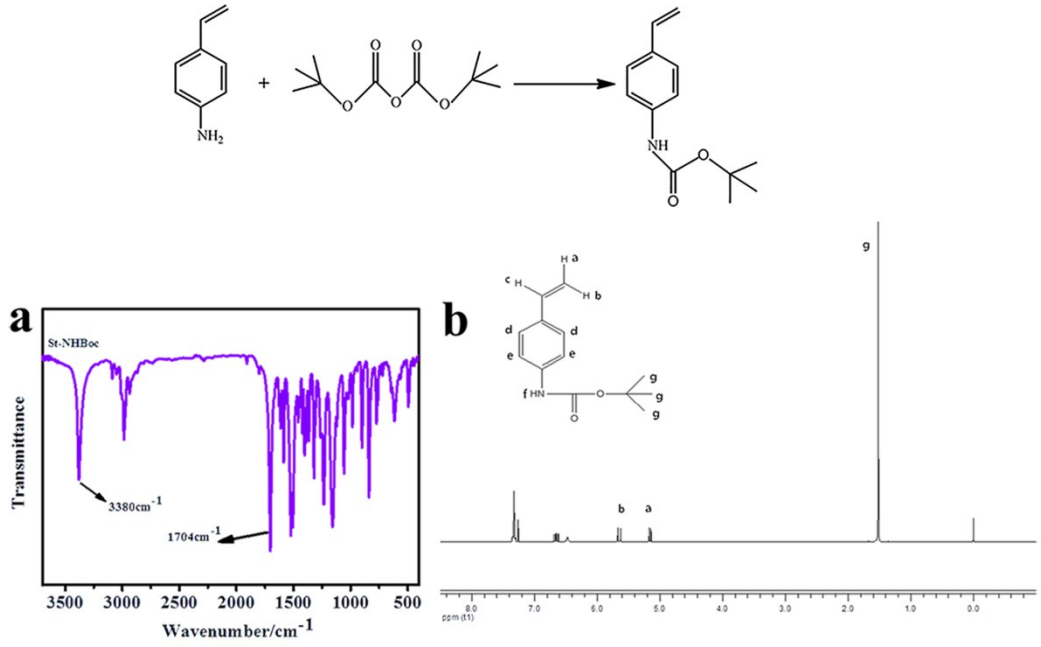

Fig. S1 (a) FT-IR spectrum of St-NHBoc. (b) ^{1}H NMR (400 MHz, δ, ppm, $CDCl_3$) spectrum of St-NHBoc: 1.5 (s, 9H, -CH_3), 5.1 (dd, 1H, =CH_2), 5.6 (dd, 1H, =CH_2), 6.6 (dd,1H, =CH-), 6.7 (s, 1H, NH), 7.3 (s, 4H, H_{ar}). The FT-IR spectrum of the St-NHBoc monomer contained typical absorption bands of protected amino group *N*-carbo-*tert*-butoxy at 1704^{-1} cm and the very sharp N-H stretching band at 3380^{-1} cm.

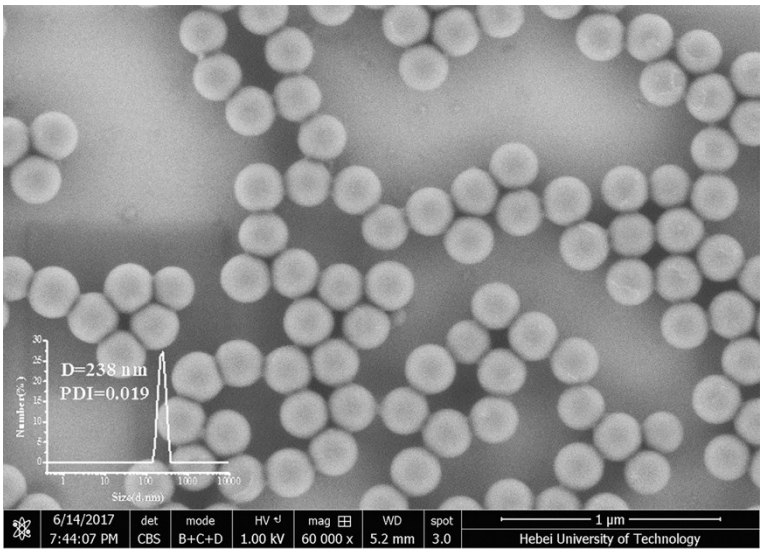

Fig. S2 SEM image of CLPS-SO_3H microspheres and average size distribution (inset).

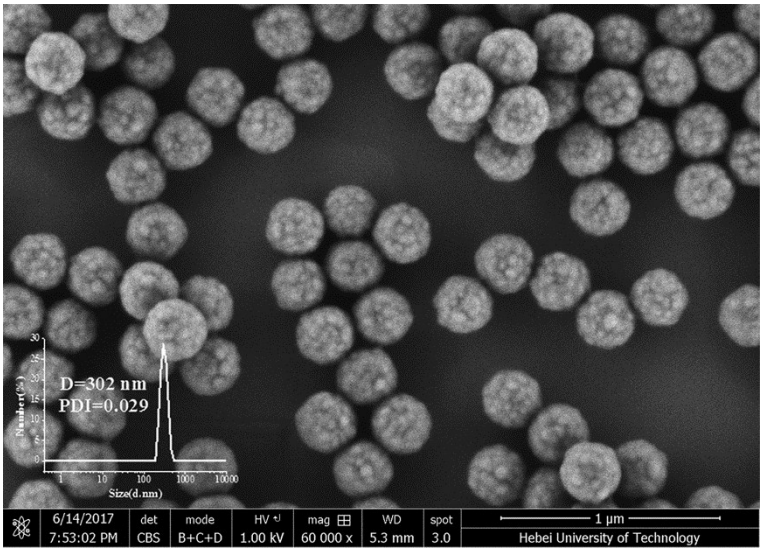

Fig. S3 SEM image of CLPS-SO_3H@SiO_2 core-shell microspheres and average size distribution (inset).

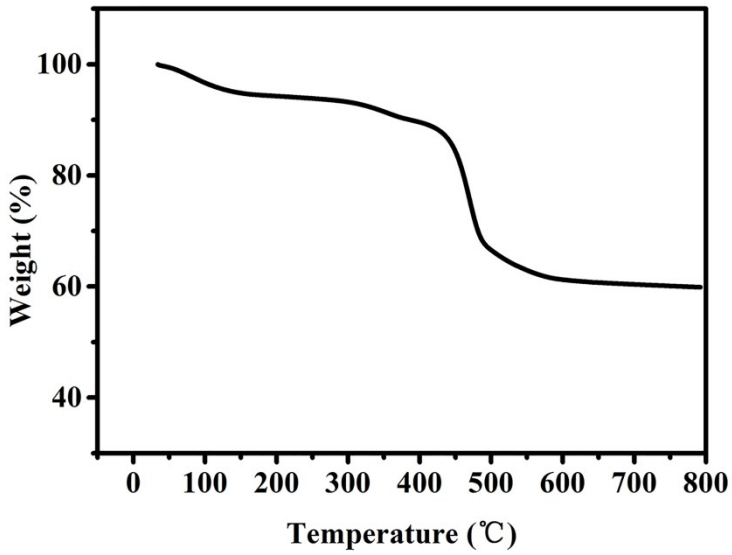

Fig. S4 The TG analysis of CLPS-SO_3H@SiO_2 core-shell composite microspheres.

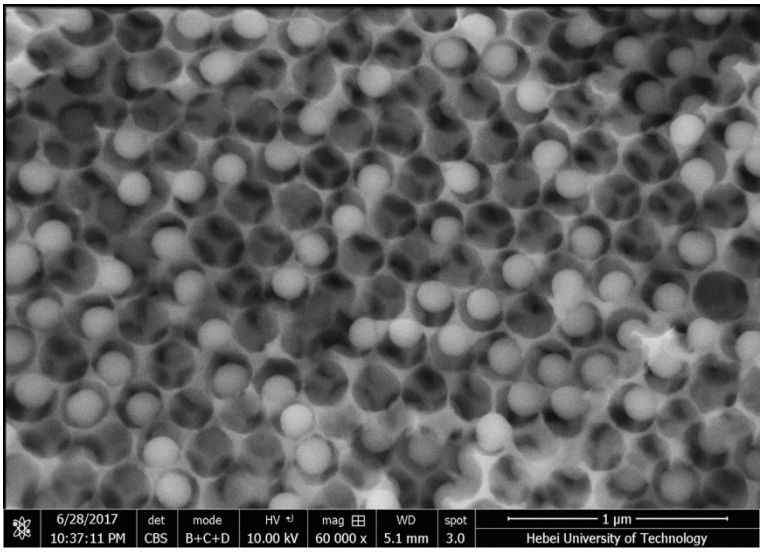

Fig. S5 SEM image of IY-SO_3H@S-NH_2 (CBS detector at 10kV).

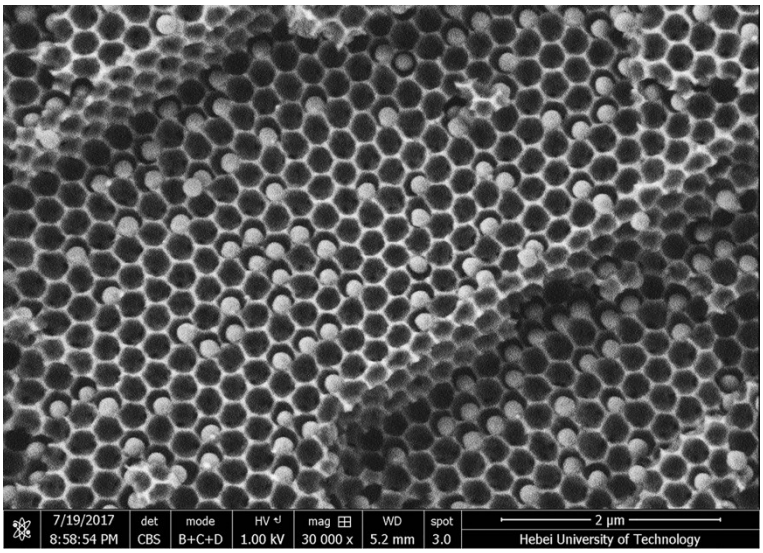

Fig. S6 SEM image of IY-SO_3H@S-NH_2 (CBS detector at 1kV).

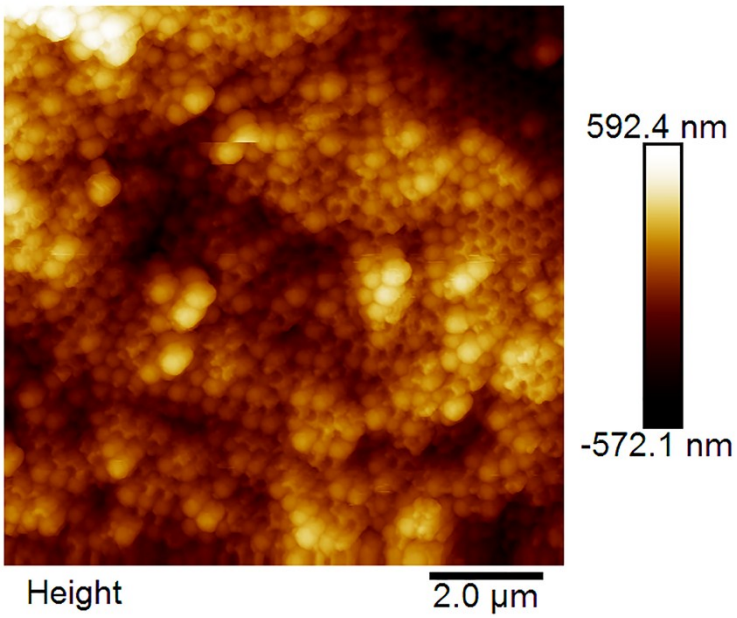

Fig. S7 AFM topography image of IY-SO_3H@SiO_2/S-NHBoc.

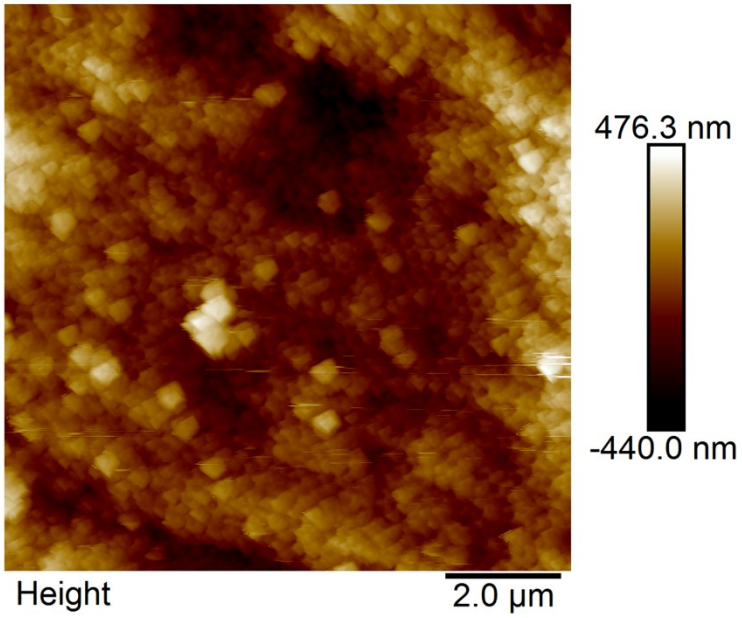

Fig. S8 AFM topography image of IY-SO_3H@S-NH_2.

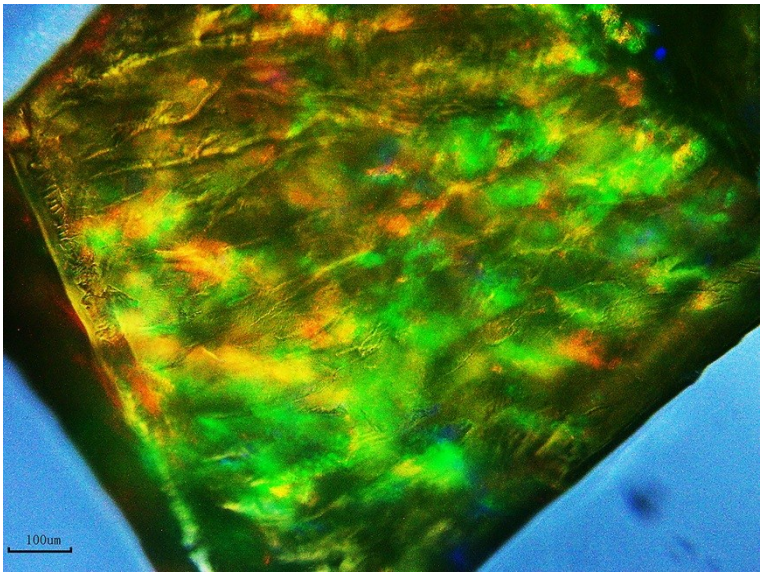

Fig. S9 Microscope image of IY-SO_3H@S-NH_2.

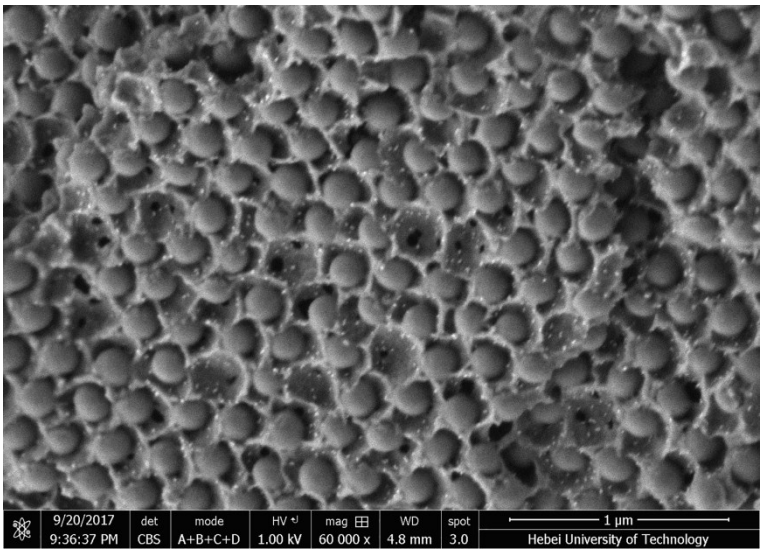

Fig. S10 SEM image of IY-SO_3H@S-NH_2/Pd.

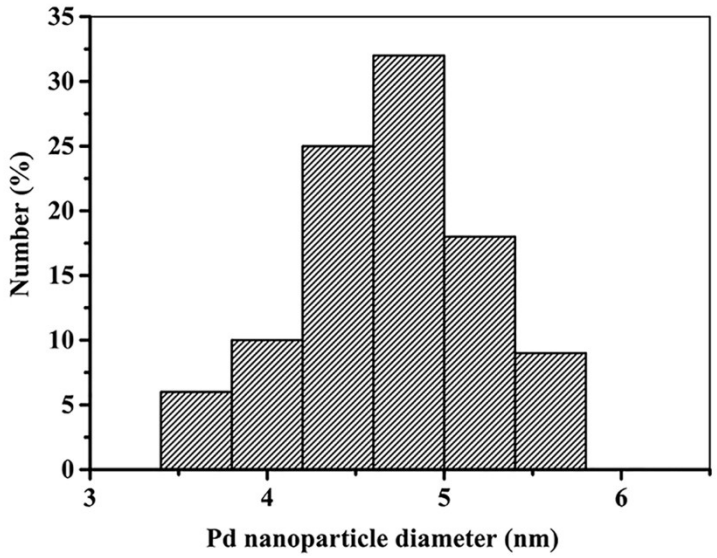

Fig. S11 The size distribution of Pd NPs on IY-SO_3H@S-NH_2 surface estimated from the TEM image via NanoMeasurer.

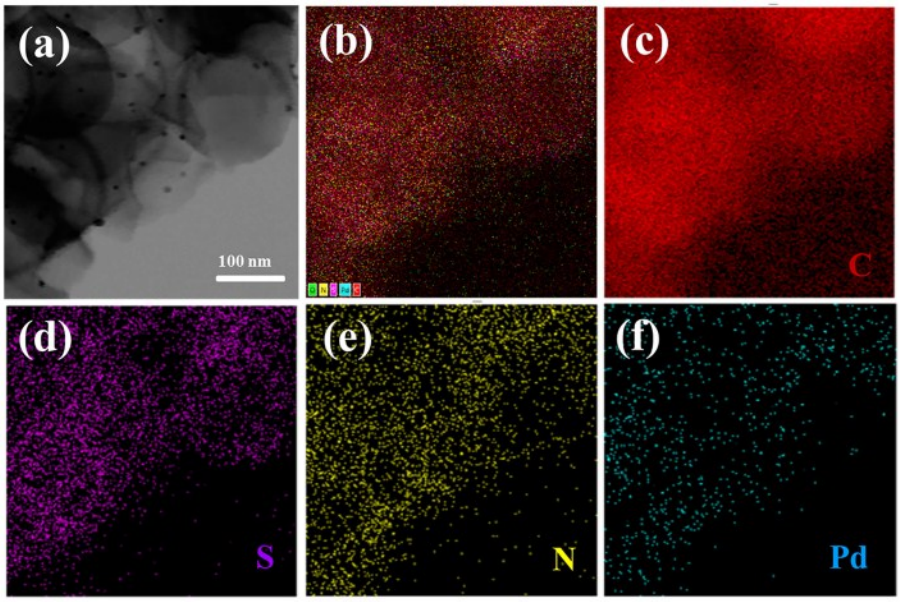

Fig. S12 (a) STEM image of IY-SO_3H@S-NH_2/Pd. EDS elemental mapping of overall (b), C (c), S (d), N (e), and Pd (f) elements in IY-SO_3H@S-NH_2/Pd.

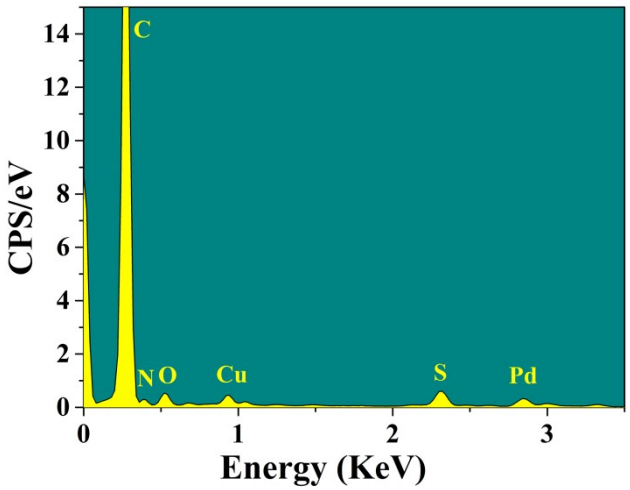

Fig. S13 EDS elemental spectrum of IY-SO_3H@S-NH_2/Pd. (Cuprum element is derived from copper mesh for sample preparation)

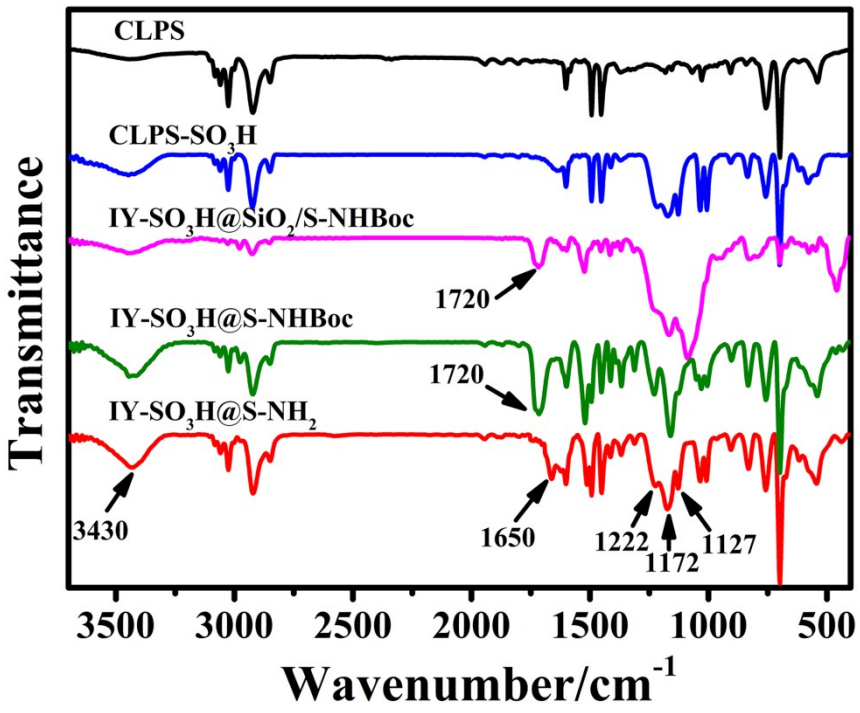

Fig. S14 FT-IR spectra of CLPS, CLPS-SO_3H, IY-SO_3H@SiO_2/S-NHBoc, IY-SO_3H@S-NHBoc, and IY-SO_3H@S-NH_2.

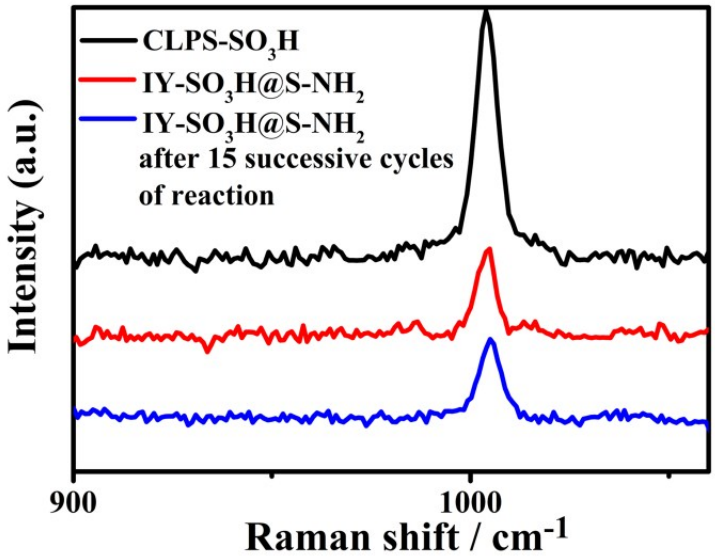

Fig. S15 UV-Raman spectra of the CLPS-SO_3H, IY-SO_3H@S-NH_2, and IY-SO_3H@S-NH_2 after 15 successive cycles of reaction.

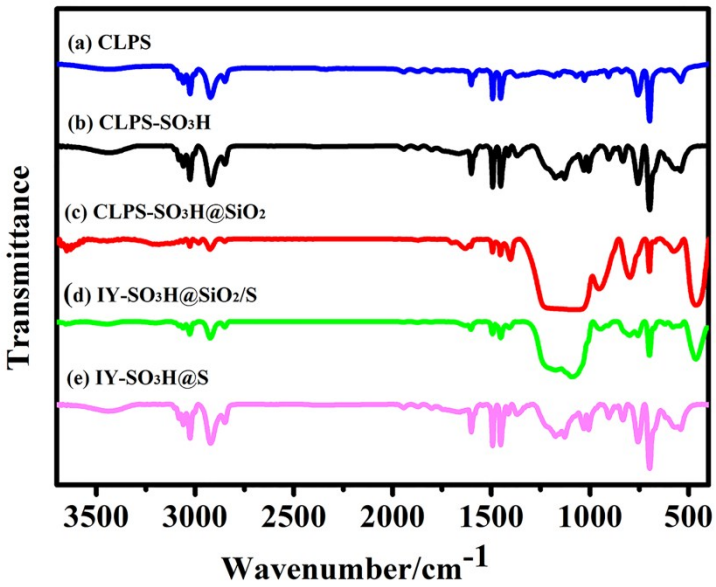

Fig. S16 FT-IR spectra of preparation process corresponding materials of IY-SO_3H@S.

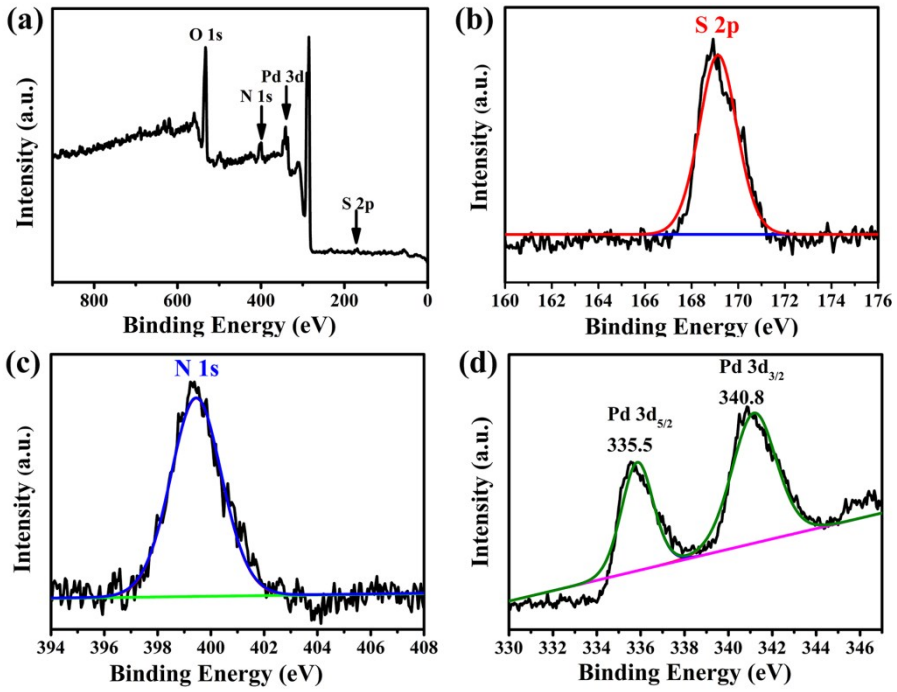

Fig. S17 (a) XPS wide-scan of the IY-SO_3H@S-NH_2/Pd, (b) S 2p core-level spectrum of the IY-SO_3H@S-NH_2, (c) N 1s core-level spectrum of the IY-SO_3H@S-NH_2, and (d) Pd 3d core-level spectrum of the IY-SO_3H@S-NH_2/Pd.

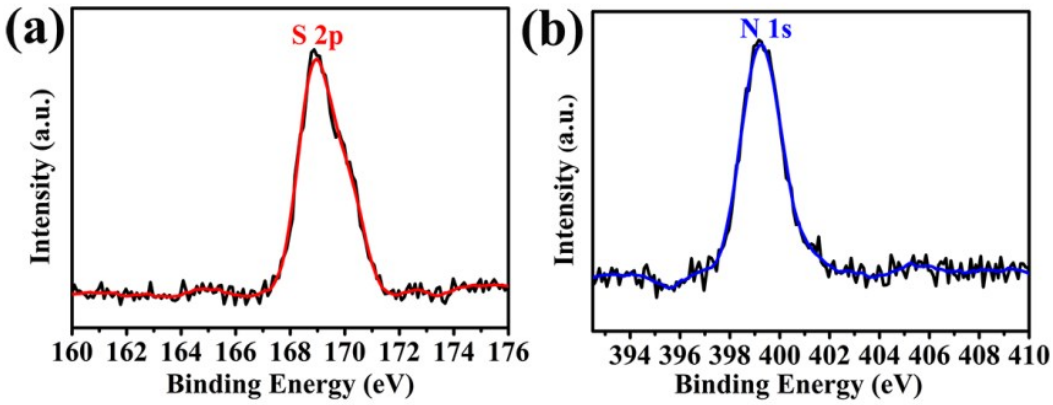

Fig. S18 S 2p (a) and N 1s (b) core-level spectrum of the IY-SO_3H@S-NH_2/Pd.

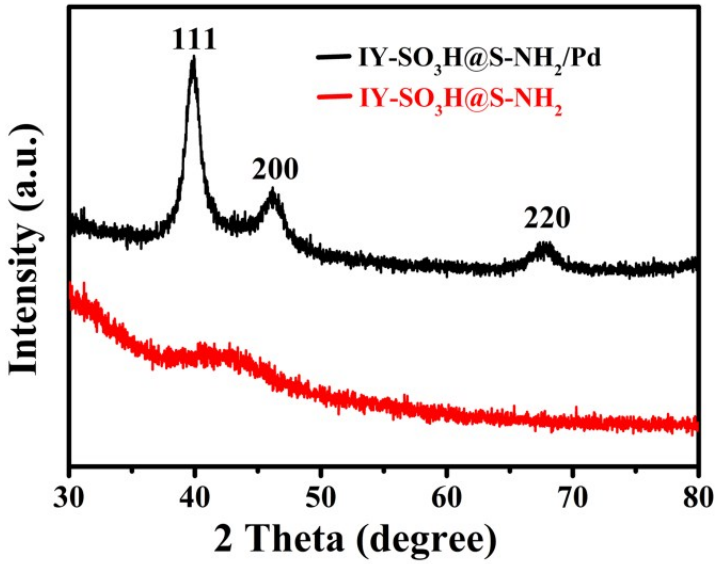

Fig. S19 XRD patterns of IY-SO_3H@S-NH_2 and IY-SO_3H@S-NH_2/Pd.

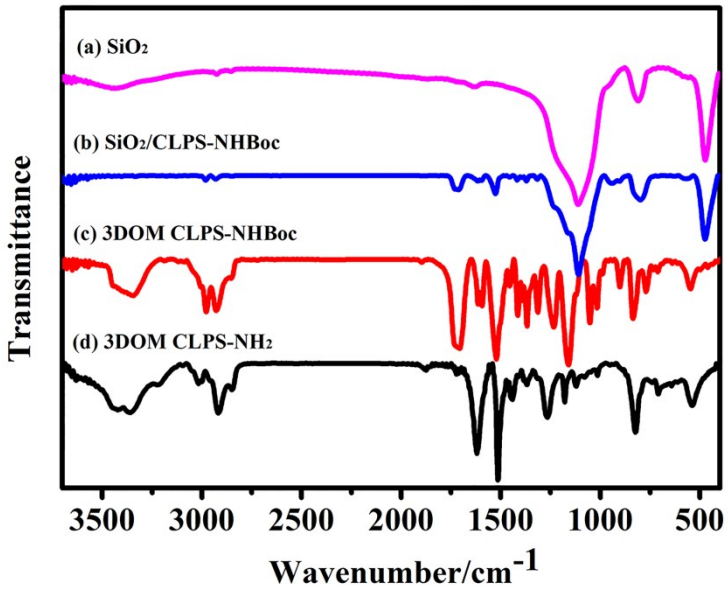

Fig. S20 FT-IR spectra of preparation process corresponding materials of 3DOM CLPS-NH_2.

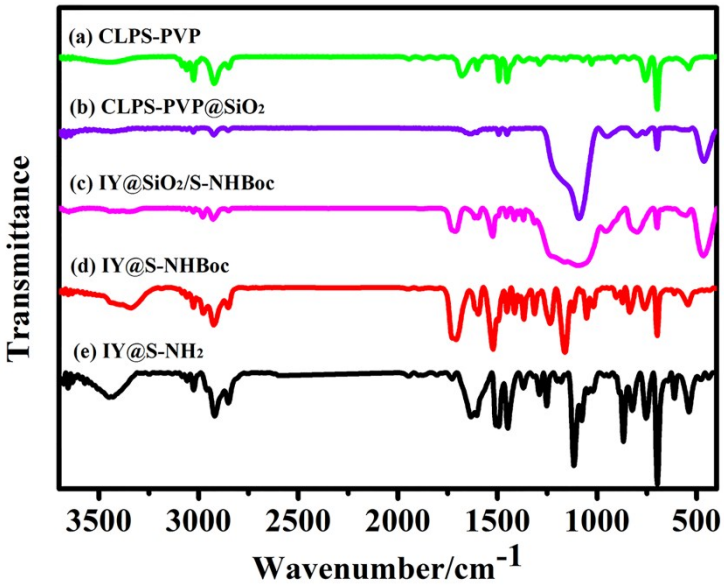

Fig. S21 FT-IR spectra of preparation process corresponding materials of IY@S-NH_2.

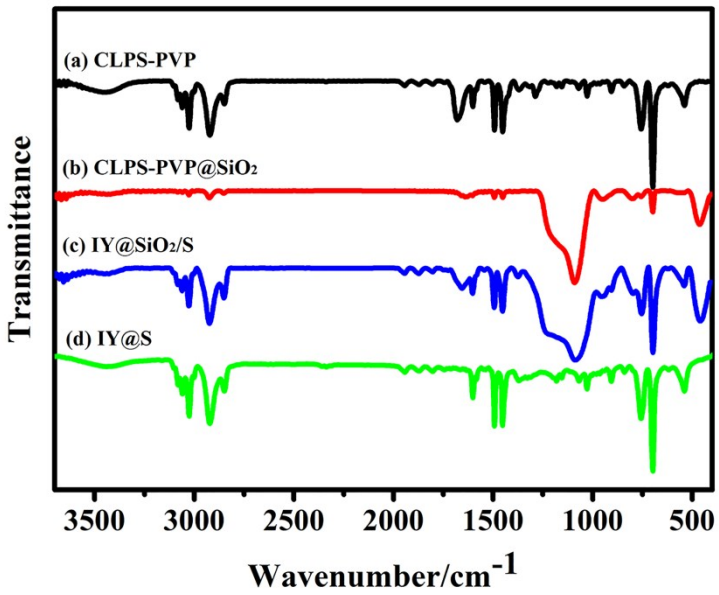

Fig. S22 FT-IR spectra of preparation process corresponding materials of IY@S.

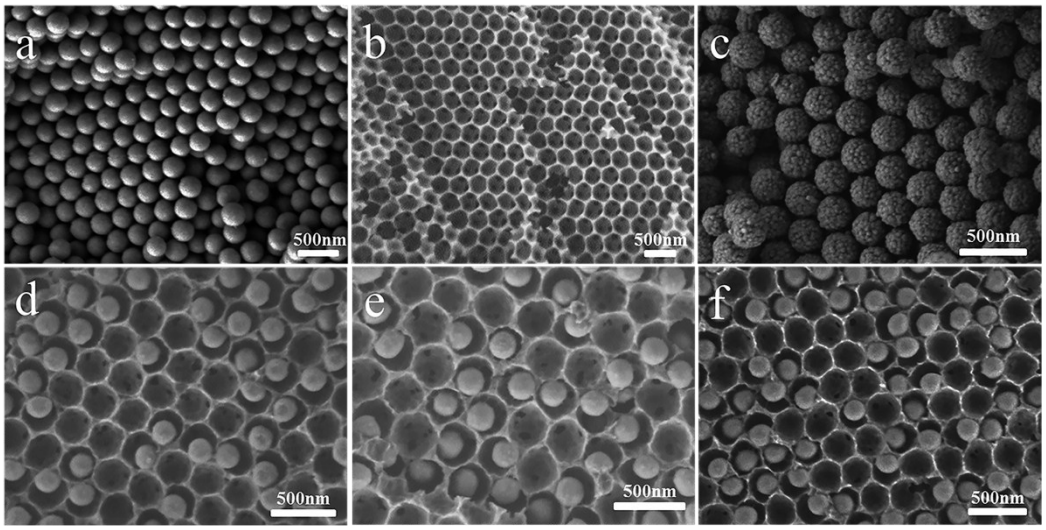

Fig. S23 SEM images of (a) SiO_2 CCTs; (b) 3DOM CLPS-NH_2; (c) CLPS-PVP@SiO_2 CCTs; (d) IY@S-NH_2; (e) IY@S; (f) IY-SO_3H@S.

Table S1. The acidic and basic parameters of various solid catalysts

Entry	Catalyst	S content (mmol/g)[a]	Acid sites (mmol/g)[b]	N content (mmol/g)[a]	Base sites (mmol/g)[b]
1	CLPS-SO_3H	1.82	1.79	0	0
2	3DOM CLPS-NH_2	0	0	7.52	7.48
3	IY@S-NH_2	0	0	2.43	2.40
4	IY@S	0	0	0	0
5	IY-SO_3H@S	1.04	0.93	0	0
6	IY- SO_3H@S-NHBoc	1.03	0.92	2.51	0
7	IY- SO_3H@S-NH_2	1.05	0.95	2.49	2.18

[a] Measured by elemental analysis. [b] Measured by acid-base titration.

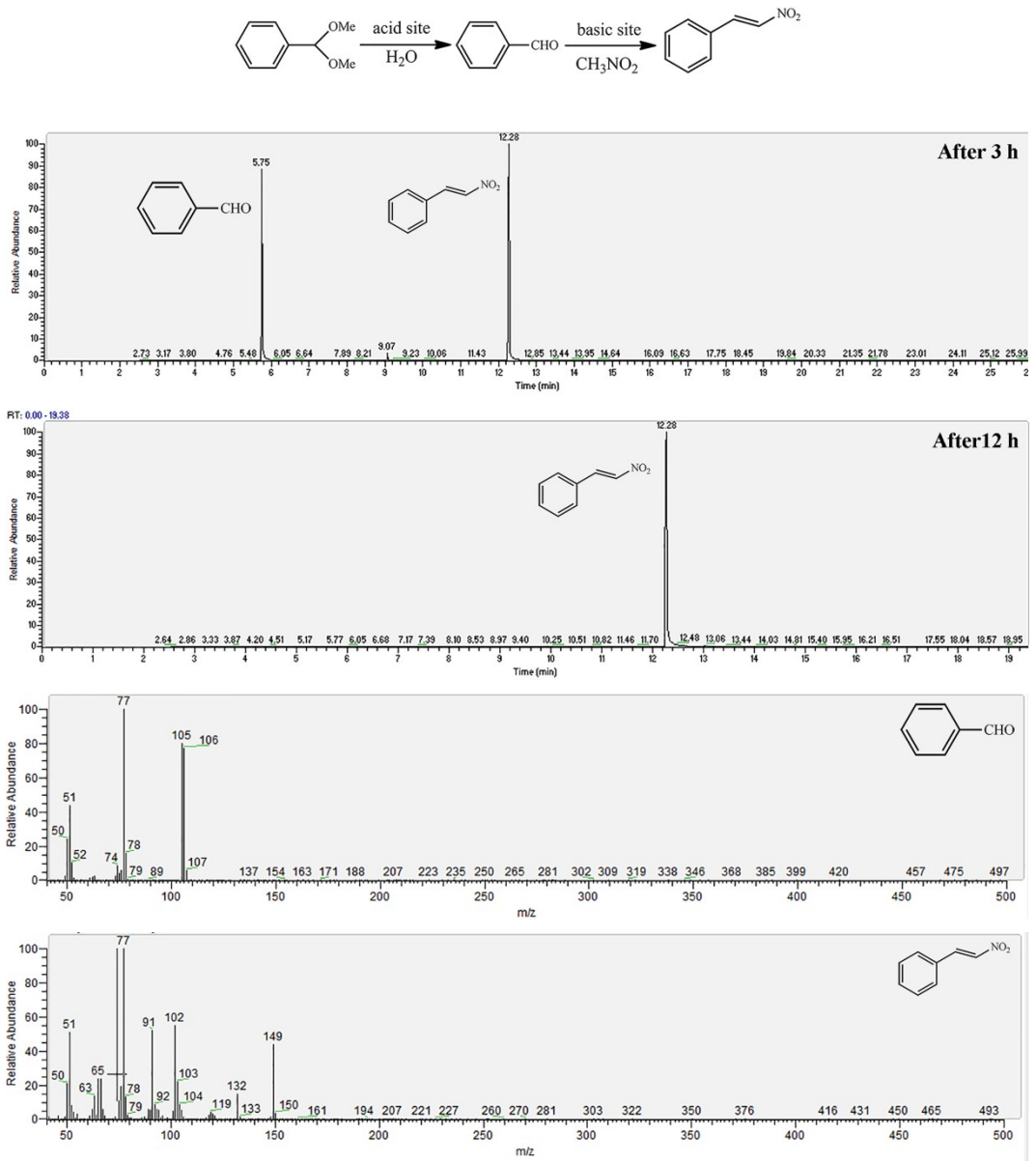

Fig. S24 GC-MS results of deacetalization-Henry reaction after 3 h and 12 h (IY-SO_3H@S-NH_2). It is seen that the bifunctional IY-SO_3H@S-NH_2 nanoreactor can catalyze the cascade reactions completely after 12 h.

Meanwhile, we also designed a deactivation experiment to further investigate the stability of the IY-SO_3H@S-NH_2. The solid 3D integrated nanoreactor was removed after 3 h was conducted, and then the mother liquor was allowed to react for another 9 h under identical reaction condition. No significant change in either the conversion of benzaldehyde or the yield of *β*-nitrostyrene was observed, demonstrating the absence of leaching and a homogeneous reaction.

The catalytic deacetalization-Henry cascade reaction process occurring in the IY-SO_3H@S-NH_2 is illustrated in Fig. 2b. The reagents (nitromethane and benzaldehyde dimethyl acetal) must diffuse through the encapsulated yolks,

and its conversion into the intermediate species (benzaldehyde) is catalyzed by -SO_3H groups on the encapsulated yolks. Subsequently, the intermediate species will pass the hollow chamber that offers a confined environment. Ultimately, they reach the interconnected shell and their conversion into the final product (β-nitrostyrene) is catalyzed by -NH_2 groups on the interconnected shell. The appropriate location of both the acidic and basic functional groups in a 3D-IYS nanoreactor can shorten the reaction pathway and enhance the synergistic effects. Meanwhile, the integrated yolk-shell unit that interconnected with each other provides a longer cycling time for reaction species.

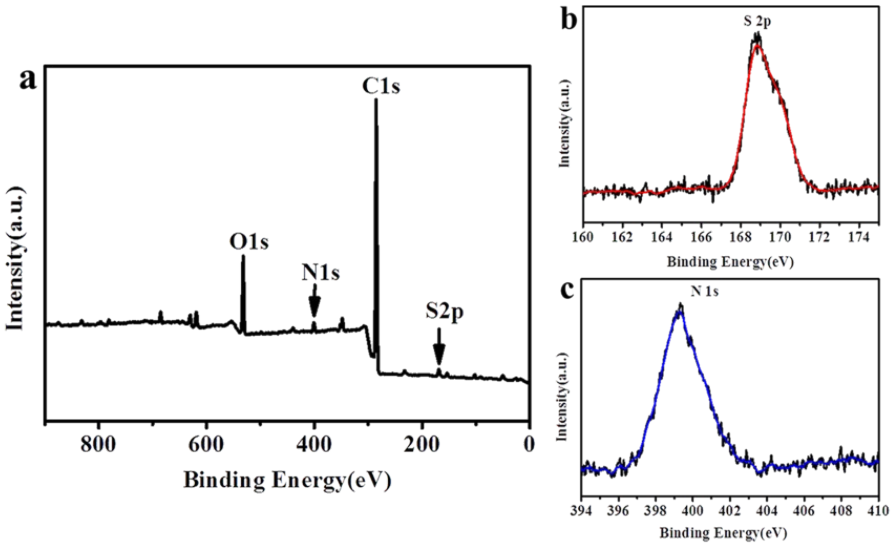

Fig. S25 (a) XPS wide-scan, (b) S 2p and (c) N 1s core-level spectra of the IY-SO_3H@S-NH_2 after 15 successive cycles.

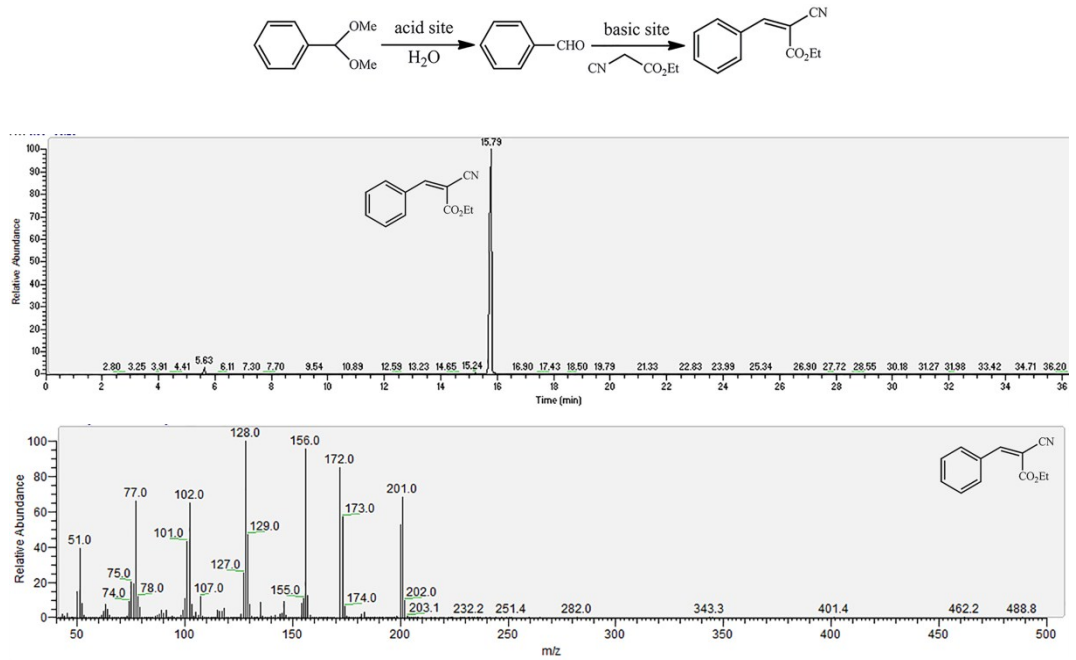

Fig. S26 GC-MS results of deacetalization-Knoevenagel condensation reaction.

Similarly, the bifunctional IY-SO_3H@S-NH_2 was used in the acid-base catalyzed one-pot cascade deacetalization-Knoevenagel reaction and showed excellent catalytic activity. This reaction sequence is composed of two separate steps: the conversion of benzaldehyde dimethyl acetal into benzaldehyde by the acid sites and benzaldehyde condensation with ethyl cyanoacetate to give the final product by the base sites. The results show that the bifunctional IY-SO_3H@S-NH_2 nanoreactor can catalyze the cascade reactions completely with >99% conversion for the starting reactants and 98% yield for the target products. Such an excellent catalytic performance is mainly attributed to the spatially separated active sites, continuously interconnected windows, 3D integrated effect and the movable encapsulated yolks of the multifunctional nanocatalyst system. These results confirm that such a 3D-IYS nanostructure is excellent as a versatile acid-base bifunctional nanoreactor for heterogeneous catalytic reactions.

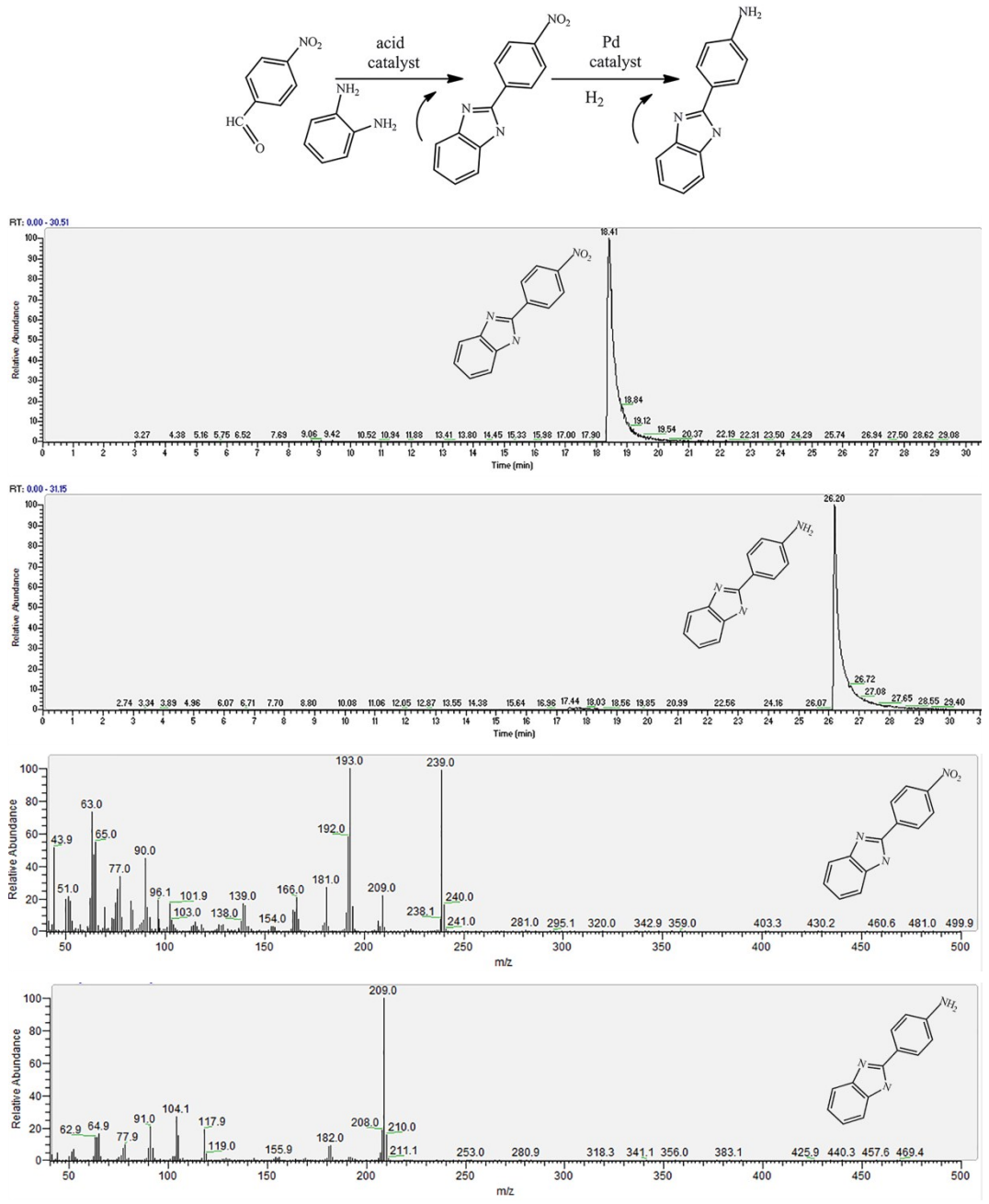

Figure S27. GC-MS results of synthesis of the 2-(4-aminophenyl)-1*H*-benzimidazole. It is seen that both the acidic catalysis and hydrogenation reaction is carried out completely.

The as-synthesized IY-SO_3H@S-NH_2/Pd can be used as nanoreactors for cascade reactions, the synthesis of 2-(4-aminophenyl)-1*H*-benzimidazole from 4-nitrobenzaldehyde and 1,2-phenylenediamine. This reaction sequence is composed of acidic catalysis and catalytic hydrogenation. 2-(4-aminophenyl)-1*H*-benzimidazole is a key intermediate in the syntheses of benzimidazole derivatives which have antiviral, antiulcer, and anticancer properties. As expected, after both the acidic catalysis and hydrogenation steps, >99%

conversion of the reactant 4-nitrobenzaldehyde and 97% yield of the desired product 2-(4-aminophenyl)-1*H*-benzimidazole were obtained.

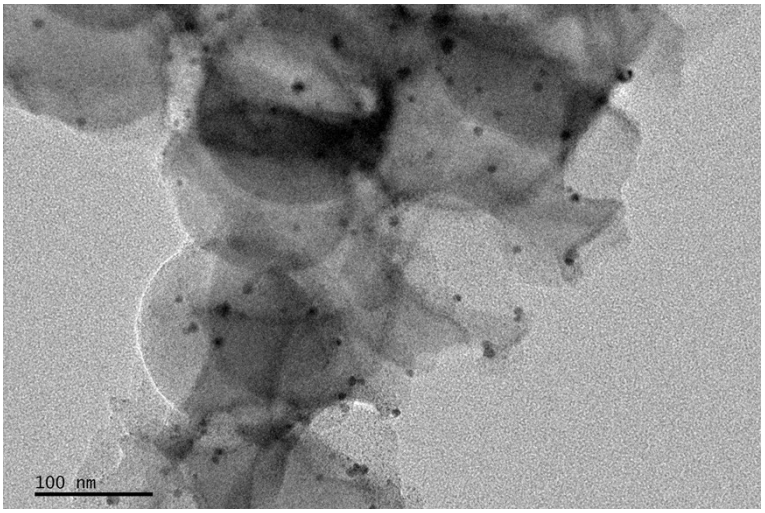

Fig. S28 TEM image of Y-SO_3H@S-NH_2/Pd after 5 successive cycles.

The TEM image of IY-SO_3H@S-NH_2/Pd after 5 repeating catalytic cycles reveals that no obvious aggregation of Pd NPs is visible. The catalytic results were determined by GC-MS. Hence, the versatility of this synthesis strategy towards the fabrication of 3D-IYS with the sufficiency of a multiscale range of active sites, controllable compositions, and interconnected windows structures has been successfully demonstrated.

REFERENCES

(1) Covolan, V. L.; Ruggeri, G.; Chiellini, E. Synthesis and Characterization of Styrene/Boc-*p*-Amino Styrene Copolymers. *J. Polym. Sci., Part A: Polym. Chem.* 2000, **38,** 2910-2918.
(2) Gu, J.; Wang, X.; Tian, L.; Feng, L.; Qu, J.; Liu, P.; Zhang, X. Construction of Grape-like Silica-Based Hierarchical Porous Inter-locked Microcapsules by Colloidal Crystals Templates. *Langmuir* 2015, **31,** 12530-12536.
(3) Wang, X.; Gu, J.; Tian, L.; Zhang, X. Hierarchical Porous Interlocked Polymeric Microcapsules: Sulfonic Acid Functionalization as Acid Catalysts. *Sci Rep.* 2017, **7,** 44178-44184.
(4) Zou, H.; Wu, S.; Ren, Q.; Shen, J. A Simple and Low-Cost Method for the Preparation of Monodisperse Hollow Silica Spheres. *J. Phys. Chem. C* 2008, **112,** 11623-11629.
(5) Zakhidov, A. A.; Baughman, R. H.; Lqbal, Z.; Cui, C.; Khayrullin, I.; Dantas, S. O.; Marti, J.; Ralchenko, V. G. Carbon Structures with Three-Dimensional Periodicity at Optical Wavelengths. *Science* 1998, **282,** 897-901.

(6) He, H.; Zhong, M.; Konkolewicz, D.; Yacatto, K.; Rappold, T.; Sugar, G.; David, N. E.; Geld, J.; Kotwal, N.; Merkle, A.; Matyjaszewski, K. Three-Dimensionally Ordered Macroporous Polymeric Materials by Colloidal Crystal Templating for Reversible CO_2 Capture. *Adv. Funct. Mater.* 2013, **23,** 4720-4728.

Table S2. Comparing the catalysis efficiency of different reported acid-base bifunctional catalysts in the cascade reactions

Catalyst	Catalyst Structure and composition	-NH_2 content	-SO_3H or -COOH content	TOF_{-NH2}	Conversion (%)	Yield of 3 (%)	Reusable (run) and Yield of 3 (%)	Ref.
HSO_3-(NH_2-SBA-15)	mesoporous SBA-15	0.18 mmol/g	0.09 mmol/g	TOF 17 h^{-1}	100.0	99.5	3-(92.1%)	1
YS-NH_2@SO_3H	yolk-shell mesoporous silica nanospheres	240 μmol/g	80 μmol/g	TOF 13 h^{-1}	100	>99	3-(72%)	2
COOH-TREN	cross-linked Micelle	---	---	---	99	86	---	3
HCP-A-B	hollow hyper-cross-linked nanospheres	1.19 wt%	1.02 wt%	---	100	96	18-(94%)	4
MS-SO_3H @MS@MS-NH_2	core-shell-shell structured mesoporous silica	0.80 mmol/g	0.50 mmol/g	---	100	≈ 100	5-(≈88%)	5
PPAF-SO_3H-NH_2	porous polymeric aromatic framework	5.12 mmol/g	0.8 mmol/g	TOF 0.57 min^{-1}	100	100	8-(≈90%)	6
COOHAHN	hollow silica nanospheres	0.1 mmol/g	---	TOF 2.7 h^{-1}	>99	95	---	7
MIL-101-SO_3H-NH_2	metal–organic frameworks	---	---	---	100	97	---	8
NH_2-GO-2	GO sheets	0.714 mmol/g	1.66 mmol/g	---	96	70	6-(91%)	9
MS-A@MS-B	core–shell structured mesoporous silica	0.71 mmol/g	0.35 mmol/g	---	100	≈ 100	4-(91.0%)	10
PAF-1-$NHCH_2CH_2NH_2$–	porous aromatic frameworks	---	---	---	100	97.2	3-(≈93%)	11

SO_3H								
30-MLHM-NH_2-SO_3H	monolayered hybrid catalyst	3.2 wt%	4.2 wt%	TOF 0.7 h^{-1}	97.0	91.9	5-(87%)	12
MFI-BTEB-NH_2	organic pillared MFI zeolite	---	---	---	≈ 100	≈ 80	---	13
MMAB	mesoporous silica	1.744 wt%	2.256 wt%	---	≈ 100	95	5-(91%)	14
PMO-SO_3H-NH_2	periodic mesoporous organosilicas	1.79 mmol/g	1.10 mmol/g	---	100	97.5	---	15
SAMSN-AP	mesoporous silica nanoparticles	0.35 mmol/g	0.35 mmol/g	TOF 3.26 h^{-1}	100	97.7	5-(96.8)	16
IY-SO_3H@S-NH_2	**three-dimensional integrated yolk-shell**	**2.49 mmol/g**	**1.05 mmol/g**	**TOF 14.4 h^{-1}**	**100**	**>99**	**15-(83%)**	**This work**

REFERENCES

(1) Wang, Z.; Yu, T.; Zaera, F. Synthesis of Solid Catalysts with Spatially Resolved Acidic and Basic Molecular Functionalities. *ACS Catal.* **2018,** *8*, 2870-2879.

(2) Yang, Y.; Liu, X.; Li, X.; Zhao, J.; Bai, S.; Liu, J.; Yang, Q. A Yolk-Shell Nanoreactor with a Basic Core and an Acidic Shell for Cascade Reactions. *Angew. Chem. Int. Ed.* **2012,** *51*, 9164-9168.

(3) Lee, L.-C.; Lu, J.; Weck, M.; Jones, C. W. Acid-Base Bifunctional Shell Cross-Linked Micelle Nanoreactor for One-Pot Tandem Reaction. *ACS Catal*. **2016,** *6*, 784-787.

(4) Jia, Z.; Wang, K.; Tan, B.; Gu, Y. Hollow Hyper-Cross-Linked Nanospheres with Acid and Base Sites as Efficient and Water-Stable Catalysts for One-Pot Tandem Reactions. *ACS Catal.* **2017,** *7*, 3693-3702.

(5) Li, P.; Cao, C.-Y.; Liu, H.; Yu, Y.; Song, W.-G. Synthesis of Core-shell-shell Structured Acid-base Bifunctional Mesoporous Silica Nanoreactor (MS-SO_3H@MS@MS-NH_2) and its Application in Tandem Catalysis. *J. Mater. Chem. A* **2013,** *1*, 12804-12810.

(6) Merino, E.; Verde-Sesto, E.; Maya, E. M.; Iglesias, M.; Sánchez, F.; Corma, A. Synthesis of Structured Porous Polymers with Acid and Basic Sites and Their Catalytic Application in Cascade-Type Reactions. *Chem. Mater.* **2013,** *25*, 981-988.

(7) Gao, J.; Zhang, X.; Lu, Y.; Liu, S.; Liu, J. Selective Functionalization of Hollow Nanospheres with Acid and Base Groups for Cascade Reactions. *Chem. Eur. J.* **2015,** *21*, 7403-7407.

(8) Li, B.; Zhang, Y.; Ma, D.; Li, L.; Li, G.; Li, G.; Shi, Z.; Feng, S. A Strategy toward Constructing a Bifunctionalized MOF Catalyst: Post-synthetic Modification of MOFs on Organic Ligands and Coordinatively Unsaturated Metal Sites. *Chem. Commun.* **2012,** *48*, 6151-6153.
(9) Zhang, F.; Jiang, H.; Li, X.; Wu, X.; Li, H. Amine-Functionalized GO as an Active and Reusable Acid-Base Bifunctional Catalyst for One-Pot Cascade Reactions. *ACS Catal.* **2014,** *4*, 394-401.
(10) Li, P.; Cao, C.-Y.; Chen, Z.; Liu, H.; Yu, Y.; Song, W.-G. Core–shell Structured Mesoporous Silica as Acid–Base Bifunctional Catalyst with Designated Diffusion Path for Cascade Reaction Sequences. *Chem. Commun.* **2012,** *48*, 10541-10543.
(11) Zhang, Y.; Li, B.; Ma, S. Dual Functionalization of Porous Aromatic Frameworks as a New Platform for Heterogeneous Cascade Catalysis. *Chem. Commun.* **2014,** *50*, 8507-8510.
(12) Gaona, A.; Diaz, U.; Corma, A. Functional Acid and Base Hybrid Catalysts Organized by Associated (Organo)Aluminosilicate Layers for CC Bond Forming Reactions and Tandem Processes. *Chem. Mater.* **2017,** *29*, 1599-1612.
(13) Liu, B.; Wattanaprayoon, C.; Oh, S. C.; Emdadi, L.; Liu, D. Synthesis of Organic Pillared MFI Zeolite as Bifunctional Acid-Base Catalyst. *Chem. Mater.* **2015,** *27*, 1479-1487.
(14) Jun, S. W.; Shokouhimehr, M.; Lee, D. J.; Jang, Y.; Park, J.; Hyeon, T. One-pot Synthesis of Magnetically Recyclable Mesoporous Silica Supported Acid–Base Catalysts for Tandem Reactions. *Chem. Commun.* **2013,** *49*, 7821-7823.
(15) Shylesh, S.; Wagener, A.; Seifert, A.; Ernst, S.; Thiel, W. R. Mesoporous Organosilicas with Acidic Frameworks and Basic Sites in the Pores: An Approach to Cooperative Catalytic Reactions. *Angew. Chem. Int. Ed.* **2010,** *49*, 184-187.
(16) Huang, Y.; Xu, S.; Lin, V. S.-Y. Bifunctionalized Mesoporous Materials with Site-Separated Brønsted Acids and Bases: Catalyst for a Two-Step Reaction Sequence. *Angew. Chem. Int. Ed.* **2011,** *50*, 661-664.